Chapter 10
Mapping Isotopic and Dissolved Organic Matter Baselines in Waters and Sediments of the Gulf of Mexico

Jeffrey P. Chanton, Aprami Jaggi, Jagoš R. Radović, Brad E. Rosenheim, Brett D. Walker, Stephen R. Larter, Kelsey Rogers, Samantha Bosman, and Thomas B. P. Oldenburg

Abstract The *Deepwater Horizon* oil spill released petroleum hydrocarbons that were depleted in $\delta^{13}C$ and $\Delta^{14}C$ at depth into the Gulf of Mexico. Stable-carbon and radiocarbon isotopic values and high-resolution mass spectrometry were used to follow the distributions of this petroleum and to track its transformation into petrocarbon, a term used to describe crude oil or transformed crude oil following biodegradation, weathering, oxygenation, or loss of lighter components. The term petrocarbon includes oil- or methane-derived carbon assimilated or incorporated into microbial biomass or into the food web as well as degraded and undegraded petroleum constituents. Here we report (1) the increase in the relative abundance of oxygen-containing carbon compounds making up the dissolved organic matter (DOM) with increasing depth through the water column, indicating the biodegradation of DOM as it was transported to depth in the water column, (2) the finding of ^{14}C depletion in DOM indicating petrocarbon inputs, and (3) the decrease and subsequent increase of ^{14}C in the isotopic composition of sinking particles indicating the capture of petrocarbon in sediment traps. In addition, we discuss the ^{14}C depletion of

---

J. P. Chanton (✉) · K. Rogers · S. Bosman
Florida State University, Department of Earth, Ocean and Atmospheric Science, Tallahassee, FL, USA
e-mail: jchanton@fsu.edu; klrogers@fsu.edu; sbosman@fsu.edu

A. Jaggi · J. R. Radović · S. R. Larter · T. B. P. Oldenburg
University of Calgary, PRG, Department of Geoscience, Calgary, AB, Canada
e-mail: aprami.jaggi@ucalgary.ca; jagos.radovic@ucalgary.ca; slarter@ucalgary.ca; toldenbu@ucalgary.ca

B. E. Rosenheim
University of South Florida, College of Marine Science, St. Petersburg, FL, USA
e-mail: brosenheim@usf.edu

B. D. Walker
University of California, Irvine -Department of Earth System Science, Irvine, CA, USA

Now at: University of Ottawa, Department of Earth and Environmental Sciences, Ottawa, ON, Canada
e-mail: brett.walker@uci.edu; brett.walker@uottawa.ca

S. A. Murawski et al. (eds.), *Scenarios and Responses to Future Deep Oil Spills*,
https://doi.org/10.1007/978-3-030-12963-7_10

this material once it is sedimented to the seafloor and the implications for oil spill budgets of seafloor petrocarbon deposition.

Keywords Organic carbon · Sediment organic matter · Radiocarbon · Dissolved organic matter · Gulf baselines · FTICR-MS · High-resolution mass spectrometry · Ramped pyrolysis

10.1 Introduction

Establishing baseline ecosystem components and monitoring them relative to these baselines can reveal the recovery of the Gulf of Mexico marine ecosystem and the effects and relative importance of future insults to the Gulf. As Pulitzer Prize winner Jack E. Davis wrote, the *Deepwater Horizon* "milestone spill is not the greatest assault to befall Gulf nature – not even close. Every day in the Gulf is an environmental disaster, originating from sources near and far that eclipses the spill…. No place is the sum of a single tragedy or continuing ones." Davis (2017). Investigation of various carbon pools has revealed quantities and pathways of hydrocarbons released during the 2010 *Deepwater Horizon* (DWH) oil spill, as discussed in previous chapters. Here we will describe downstream effects and follow petrocarbon as it moved through the ecosystem and into three major pools of oceanic carbon in the northern Gulf of Mexico: dissolved organic matter (DOM), sinking particulate organic matter ($\mathrm{POM_{sink}}$), and sedimentary organic matter (SOM). Knowledge and monitoring of the isotopic composition of these organic components relative to their baseline values provide invaluable information regarding the Gulf's health and the potency of the anthropogenic stressors affecting it.

These three pools of organic matter play key roles in the biogeochemical cycling of carbon and other nutrients such as phosphorus, nitrogen, and sulfur. They record varying time scales of the carbon inputs to the Gulf which are responsible for secondary production, and they influence the solubility, transport, and toxicity of organic and inorganic pollutants (Kujawinski et al. 2002; Kim et al. 2004; Nebbioso and Piccolo 2013). DOM is operationally defined as the fraction that can pass through a nominal size filter (usually between 0.2 and 0.7 μm), ($\mathrm{POM_{sink}}$) is the material collected in a sediment trap (Passow et al. 2012; Yan et al. 2016), and SOM accumulates on the seafloor (Brooks et al. 2015; Schwing et al. 2017). The residence time of DOM in the ocean is on the order of thousands of years (Williams and Druffel 1987; Bauer et al. 1992, 2002; Druffel et al. 1992 1996). With a sinking velocity that varies from 68 to 553 m $\mathrm{d^{-1}}$ (Diercks and Asper 1997; Passow et al. 2012), $\mathrm{POM_{sink,}}$ reflects at time scales of short duration. In a 2000 m water column, these sinking velocities would result in a residence time of 4–30 days for POM in the water column. However, longer residence times may occur at the sea surface prior to the initiation of sinking as the exopolymeric substances that bind particles are initially somewhat buoyant (Azetsu-Scott and Passow 2004). Sedimentary organic matter, by contrast, provides a sequence of time horizons of varying duration, depending upon the sedimentation rate, and provides a record on the decadal to millennial time scale in the northern Gulf of Mexico.

Globally, the DOM pool accounts for ~662 Pg of carbon (Hansell et al. 2009), making it one of the Earth's largest active carbon pools, comparable in magnitude to atmospheric carbon dioxide load (~750 PgC; Hedges 1992). Sinking POM accounts for about 11.1 Pg of carbon exported to the ocean interior annually (Hansell 2013; Libes 2011). The part of this sinking flux which escapes complete remineralization is preserved in the sediments (~2.60 PgC yr^{-1}; Burdige and Komada 2015) and, although small in comparison, represents an important transfer between active carbon pools (fast-cycling) and geological carbon pools (cycling on millennial or greater time scales). The burial of the organic matter in the marine sediments represents an important link between the "active" biological carbon cycle in the oceans and the "inactive" carbon pool in the marine sediments, which cycle over much longer geologic time scales. In this chapter we will review some of the latest findings related to the molecular and carbon isotope (stable and radiocarbon) composition of these three pools of marine OM in the Gulf of Mexico system.

10.2 Analytical Approaches

Two approaches to define background and excursions from background will be described in this chapter. The first approach is the application of ultra-high-resolution Fourier-transform ion cyclotron resonance mass spectrometry (FTICR-MS) to explore changes in molecular-level composition of organic compounds partitioning to aqueous phase. FTICR-MS provides a combination of high resolving power and high accuracy of mass detection, facilitating the assignment of molecular formulas to individual water-soluble components extracted from DOM and SOM via solid-phase extraction without the need for prior separation by chromatographic or other methods. The second approach is the tracing of petroleum- and methane-derived carbon (petrocarbon) through the pools described above, using natural abundance stable carbon and radiocarbon isotopes ($\delta^{13}C$ and $\Delta^{14}C$, Fig. 10.1) (Stuiver and Pollach 1977; Bosman et al. 2017) and for POM_{sink}, $\delta^{34}S$.

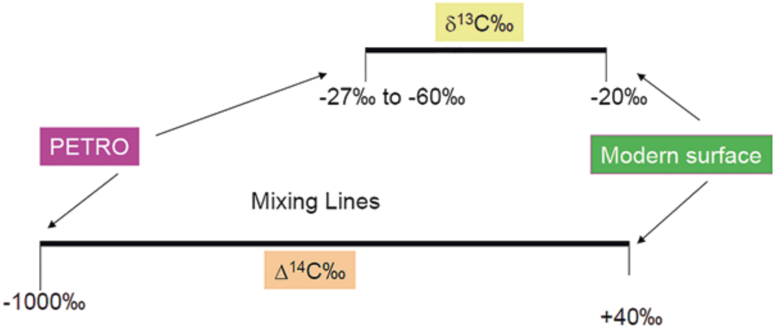

Fig. 10.1 Schematic drawing of the stable and radiocarbon two end-member mixing lines. Positions located closer to the left indicate samples containing petrocarbon, while positions located closer to the right indicate samples containing modern surface carbon in the Gulf of Mexico. (Bosman et al. 2017)

10.2.1 High-Resolution Mass Spectrometry: FTICR-MS

The pools of DOM in the water column and that extracted from the sediments by aqueous extraction (WEOM, water-extractable organic matter) encompass a cocktail of compounds with distinct molecular formulas, each of which constitutes a multitude of structural isomers, making the molecular assembly of the DOM one of the most complex and diverse organic mixtures on the planet (Dittmar and Stubbins 2013). The previously applied approaches for the characterization of this complex mixture, both dissolved in the water column and adsorbed on the sediment surface, have been constrained to the investigation of the bulk composition, with limited molecular characterization efforts (e.g., Benner et al. 1992; Ogawa et al. 2001). The application of ultra-high-resolution Fourier-transform ion cyclotron resonance mass spectrometry (FTICR-MS) provides a combination of high resolving power and high accuracy of mass detection, facilitating the assignment of molecular formulas to individual components, thereby making it sensitive to experimental processes that affect molecular-level composition (Stubbins et al. 2010). Its capability of analyzing high-molecular-weight, polyfunctional, and polar compounds makes it ideal for the characterization of dissolved organic matter in water and sediments.

FTICR-MS measures the mass to charge ratio (m/z) of an ion by measuring its cyclotron motion frequency in the influence of a magnetic field. The magnetic field, B, induces a cyclotron motion of the ions, because of the Lorentz force exerted on the ions, with mass m and a charge of q. For a given magnetic field strength, the cyclotron frequency of the ions in the ion cyclotron resonance (ICR) cell depends solely on the m/z ratio. The Bruker 12T SolariX FTICR-MS used in this study yields mass resolution of 2,000,000 at m/z 400, with maximum typical error as low as 150 ppb. The high resolving power and mass accuracy offered by the FTICR-MS can determine the mass of a molecule within 0.10 mDa, even lower than the mass of an electron (0.55 mDa).

The water DOM and sediment WEOM samples were analyzed using ultra-high-resolution mass spectrometry with electrospray ionization in negative (ESI-N) ion mode. The water samples were collected using a CTD-Niskin rosette sampler at various sites in the Gulf of Mexico in the summer of 2015 onboard the RV *Weatherbird II* and RV *Justo Sierra*. The DOM from the waters was extracted using the solid-phase extraction (SPE) protocol described by Dittmar et al. (2008). The extracts were then analyzed using FTICR-MS. The sediment samples were collected using an MC-800 multicoring system (Ocean Instruments, San Diego, CA, USA) from the Gulf of Mexico in the summer of 2015 onboard the RV *Weatherbird II* and RV *Justo Sierra*. Each sediment core was refrigerated at ~4 °C until subsampled by layer extrusion at 2 mm depth intervals, using a calibrated threaded-rod extrusion device (Verschuren 1993). The 2 mm extruded sediment samples were combined evenly for the top 15 cm of the sediment depth, to make a final dry weight of 23 g for each sampled site. The samples were then transferred into pre-combusted glass fiber thimbles (30 × 100 mm, Whatman) and Soxhlet extracted with 250 mL of deionized water for 48 h at 97 °C (Calgary altitude ~1100 m).

10.2.1.1 Stable Isotope Analysis

For both POM pools and SOM, a flash combustion elemental analyzer was used to convert organic molecules to CO_2 in a stream of He. This stream of He was continuously monitored for stable isotope ratios using a Finnigan Delta XP isotope ratio mass spectrometer. For purposes of interlaboratory comparison, laboratory reference materials of isotopic composition known relative to international standards are treated in the same way as the samples. All values are reported relative to the Vienna Pee Dee Belemnite (VPDB) standard with analytical precision of generally 0.2‰.

Methods for the determination of dissolved organic carbon (DOC) concentrations and isotopic composition are described in detail in Walker et al. (2017) and Beaupré et al. (2007). Briefly, UV photochemical oxidation (UVox) was used to convert dissolved organic molecules to aqueous $CO_{2.}$ Prior to UV oxidation, it is necessary to remove existing dissolved inorganic carbon (DIC) from samples. Thus, samples were acidified with 1 mL of H_3PO_4 and sparged with He to carry out gaseous CO_2. Once samples were free of naturally occurring DIC, UV oxidation was employed, and the samples were sparged with He to remove the resultant CO_2. The CO_2 resulting from oxidation of the DOM was split 200–400 μg C aliquots for radiocarbon and 12–30 μg C aliquots for stable isotope analysis.

For DOC, equilibrated splits of sample CO_2 gas purified from DOC treated with UV oxidation were cryogenically isolated into 3 mm Pyrex tubes and sealed on a vacuum line. These 3 mm glass ampules were then placed in UHP He-flushed 12 mL Exetainer® vials and cracked in the He atmosphere. The resultant mixture of CO_2 and He was then introduced to a Finnigan Delta Plus isotope ratio mass spectrometer via a continuous flow Gas Bench II sample preparation system.

10.2.1.2 Radiocarbon Analysis

For all DOM, POM, and SOM samples, cryogenically purified CO_2 gas from sample UV oxidation or closed-tube combustion was cryogenically purified on a vacuum line and manometrically quantified. Equilibrated sample CO_2 gas splits were then catalytically reduced to graphite on a Fe catalyst either by the H_2 reduction method (Vogel et al. 1987) or the sealed-tube Zn method (Xu et al. 2007; Walker and Xu 2019). Graphite was then packed into ion source targets and sputtered with Cs^{+2} to form a negatively charged carbon ion beam for the detection of ^{14}C in an accelerator mass spectrometer (AMS). Radiocarbon analysis reported in this chapter was carried out in several AMS labs. POM and SOM $\Delta^{14}C$ measurements were made at the National Ocean Sciences Accelerator Mass Spectrometer (NOSAMS), the Center for Applied Isotopic Studies at the University of Georgia, or Lawrence Livermore National Lab. Total DOM $\Delta^{14}C$ measurements were performed at the University of California, Irvine Keck Carbon Cycle AMS Lab.

10.3 FTICR-MS

10.3.1 Geochemical Characterization of the FTICR-MS Composition of the Baseline Water Column Profile (at Multiple Depths) from Northern Gulf of Mexico

The identified peaks in the ESI-N FTICR-MS mass spectra of the analyzed water DOM extracts extended on average from *m/z* 200 to 750 with the spectra being dominated by four compound types: NO_x, N_2O_x, N_3O_x, and O_x, where x denotes variable number of oxygen (from 5 to 16). The DOM spectra show a Gaussian distribution was observed for the relative abundance of the individual heteroatom-dominated compound classes with increasing heteroatom number. The homogeneity in the compound class distribution of DOM and the uniform Gaussian distribution is expected, considering the constant diagenetic transformations ongoing in the marine ecosystems due to microbial degradation and photooxidation and longer residence time of dissolved fraction of organic matter pool (Opsahl et al. 1999; Spencer et al. 2009; Stubbins et al. 2010; Tarr et al. 2016).

The DOM spectra were enriched in multi-oxygenated species, with the classes $O_{2–18}$ having the highest contribution to the relative intensity of all compound classes present in the DOM, as also observed in previous studies analyzing DOM from natural systems (Fig. 10.2a) (Koch et al. 2007; Sleighter and Hatcher 2008). Across different sampling depths, these multi-oxygenated species exhibited a trend of the increasing intensity and number of oxygen atoms in the O_x compound class from surface to bottom of the water column (Fig. 10.2a). This trend suggests that the overall concentration of the DOM extracted using SPE is higher in the bottom waters compared to the surface. The published literature on DOM across marine ecosystems around the world (e.g., Koch et al. 2005; Mentges et al. 2017; Stubbins and Dittmar 2015) have also reported seeing a similar abundance gradient with depth.

The double bond equivalent (DBE) distribution of the O_x classes for the analyzed DOM spectra in ESI-N mode, when normalized to its relative intensity, shows a unit shift trend of the DBE with maximum relative intensity for each plotted class, similar to the pattern observed by Bae et al. (2011) for water column DOM. This increase of the intensity and inferred abundance of the O_x class group with an increase in sampling depth, combined with the pattern increase of DBE and carbon number by 1 unit, per addition of 2 oxygen atoms, suggests that the increase is due to transformation, resulting in the addition of -COOH groups. Previous characterization of deep marine DOM using NMR has also attributed the increased abundance of oxygen-containing species to the carboxylic functionality (Helms 2012; Stubbins and Dittmar 2015). Some of these compounds have been identified as microbially derived carboxylic-rich alicyclic molecules (CRAM) having a cyclic backbone with high carboxylation levels (Hertkorn et al. 2006). Hertkorn et al. (2006) also proposed that the deep-ocean refractory DOM was comprised of CRAM, which accounts for nearly 8% of the DOM pool.

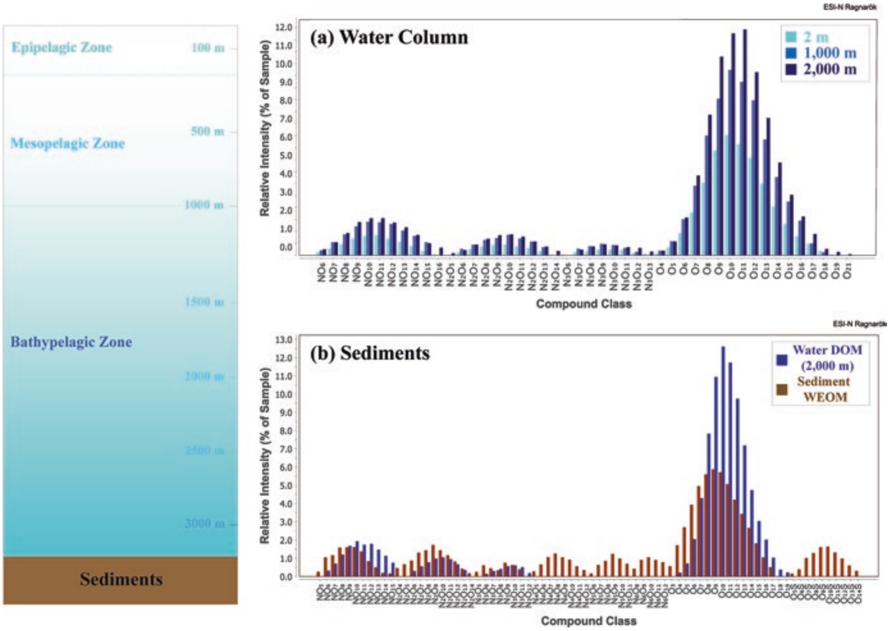

Fig. 10.2 FTICR-MS ESI-N compound class distribution of (**a**) water DOM along the water column at 2 m, 1000 m, and 2000 m, and (**b**) comparison of the water DOM (at 2000 m) and sediment WEOM for northern Gulf of Mexico data is publicly available through the Gulf of Mexico Research Initiative Information and Data Cooperative (GRIIDC) at https://data.gulfresearchinitiative.org R4.x267.179:0003

The increase in the relative abundance of the carboxyl group making up the DOM with increasing depth through the water column; indicates that biodegradation is occurring as DOM is transported to depth in the water column. Dittmar and Stubbins (2013) suggested that the increase in the species containing -COOH group with depth could be attributed to the corresponding depletion of labile DOM within the bathypelagic ocean, resulting in the production of an oxidized pool. The slow settling of this oxidized pool of DOM over thousands of years toward the bottom of the ocean would explain the increased relative intensity of multi-oxygenated species (Dittmar and Stubbins 2013).

10.3.2 Geochemical Characterization of the FTICR-MS Composition of the Baseline Sediment WEOM from Northern Gulf of Mexico

Bulk SOM and sediment DOM can itself be categorized into three operationally defined phases: pore water organic matter, water-extractable organic matter (WEOM) from the solid phase, and organic solvent-extractable organic matter from the solid phase (Chen and Hur 2015). The aqueous Soxhlet extraction of sediment provides a more diverse pool of organics with fresher and less degraded constituents than the pore water organics extracted with conventional methods (Schmidt et al. 2014). The analysis of sedimentary organic matter using WEOM therefore offers a more comprehensive picture and a better alternative for sedimentary DOM characterization, especially when FTICR-MS analysis of pore water is limited by the sample volume availability.

The identified peaks in the ESI-N FTICR-MS mass spectra of the analyzed water extracts extended on average from *m/z* 150 to 650 with the spectra being dominated by eight compound types: NO_x, N_2O_x, N_3O_x, N_4O_x, N_5O_x, N_6O_x, O_x, and SO_x. The sediment WEOM spectra are enriched with nitrogen-containing compounds, containing up to six nitrogen heteroatoms with a wider compositional range compared to the water DOM extracts (Fig. 10.2b). The elevated nitrogen-containing species in the sediment WEOM suggests a release of molecules during water extraction, most likely from the protein-rich microbial cell walls present in the sediment. Schmidt et al. (2014), however, established this phenomenon to be minor for extraction of WEOM from sediments using Soxhlet, and insufficient to explain the increase in peptide-like compounds, thereby likely suggesting that these compounds are likely being produced in situ in the sediments. These nitrogen-rich moieties in the sediment WEOM could be related to melanoidins, which are formed by the condensation reaction between the sugars and amino acids via the Maillard or “browning” reaction (Hedges 1978). The high nitrogen-containing melanoidins produced in the marine waters have high affinities for clay material surfaces and bind to the suspended clay particulates forming aggregates, which sink through the water column adding to the sediment WEOM pool (Hedges 1978). This sinking of melanoidin-clay aggregates along the water column could explain absence of the melanoidin signature in the water DOM.

In addition to the nitrogen-containing moieties, the sediment WEOM contain a higher concentration of sulfur-containing compounds, which are likely formed by natural vulcanization reactions during sediment diagenesis, incorporating inorganic sulfur (from seawater sulfate reduction in the anaerobic zone) into lipids and carbohydrates (Wakeham et al. 1995; Aycard et al. 2003).

10.3.3 Continuum Between Water Column and Sediments

The water DOM extracts showed high relative intensities of oxygen-containing moieties, double bond equivalents, and carbon number values, compared to the sediment WEOM extracts, which showed a high relative intensity of nitrogen-containing compound classes. The lower carbon number and DBE values of the sediment WEOM in contrast to the aquatic DOM (Jaggi 2018) likely represent the low-molecular-weight intermediates from the series of hydrolytic, fermentative, and eventually respiratory processes taking place in the sediments (Henrichs 1992;

Arnosti et al. 1994; Burdige and Gardner 1998). The differences in the residence time of the DOM were also observed in the spectra between aquatic DOM and sediment WEOM. Whereas the aquatic DOM creates homogenous spectra owing to the slower transformations, dilutions, and longer residence times, the sediment WEOM show a higher variability in the composition between different locations, owing to the relatively faster deposition.

The biological processes are more robust in the water column resulting in the smoothing of the organic signature, while the anoxic conditions in the sediments restrict degradation, contributing to the preservation of more information regarding diagenetic changes and contaminations seen by a region (Emerson and Hedges 1988; Hedges and Keil 1995). For instance, an increased organic load in a natural setting, like an oil spill, would increase the aggregation of DOM in the water column with the suspended particles and diverse community of bacteria, phytoplankton, and protozoans, creating a sinking flux of organic matter (Turley and Stutt 2000). Such phenomenon of the sinking of the formed organic aggregates generates an action of "cleaning the water column" by moving the organics to the ocean floor. The characterization of organics in the sediments better preserves the signatures of different input sources.

10.4 Stable and Radiocarbon Isotopic Composition of Gulf of Mexico Organic Matter Pools

10.4.1 Dissolved Organic Carbon

A recent study by Walker and co-authors (2017) produced the first total dissolved organic carbon (DOC) $\Delta^{14}C$ and $\delta^{13}C$ water column profiles in the Gulf of Mexico. These data provide us with both baseline DOC concentrations and carbon isotopic data but also insight into the cycling of DOM in this key ocean region. DOC concentrations from most station depths in the Gulf of Mexico water column closely matched previous analysis of $DO^{14}C$ from the open Atlantic Ocean adjacent to the Lesser Antilles (Druffel et al. 2016; Walker et al. 2017) (Fig. 10.3). Surface DOC isotopic data suggest primary production ($\delta^{13}C = -20.7‰$) is the predominant source of modern DOC in the surface Gulf. In the deep Gulf basin (Station P4), DOC $\delta^{13}C$ signatures range between −21.3 and −21.8‰. DOC $\Delta^{14}C$ values are slightly higher than expected from deepwater recharge sources (i.e., Caribbean and NADW). An ~11‰ offset from deep water at A20 and P4 suggests an apparent DOC ventilation time in the GOM of ~150 ^{14}C years. However, recent physical advection estimates of Gulf of Mexico basin suggest a ventilation of ~250 years (Rivas et al. 2005). This may indicate some modern deep DOC contributions from sinking particles. It is interesting to note that very low DOC $\Delta^{14}C$ values are not observed in the abyssal GOM. This is somewhat surprising given recent work

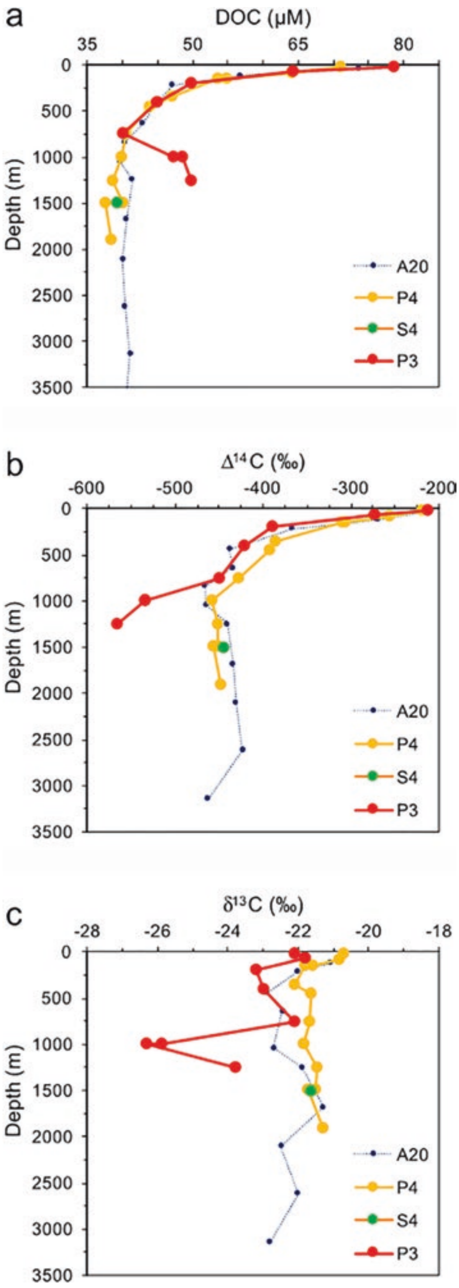

Fig. 10.3 Northern Gulf of Mexico dissolved organic carbon (DOC) concentrations (**a**) together with stable carbon ($\delta^{13}C$) (**b**) and radiocarbon ($\Delta^{14}C$) (**c**) isotopic values clearly indicate the presence of excess petrocarbon DOC at the Macondo wellhead site (P3; 28.65°N, −88.56°W) relative to offshore Gulf sites (S4; 28.04°N, −88.75°W and P4; 27.53°N, −88.75°W) and those in the Caribbean Sea (A20, Station 27, April 2012; 12.75°N, −52.33°W). For all plots, measurement uncertainties are smaller than the symbols. All Gulf samples were collected in July 2014 (R/V Pelican, PE15-01). (Data are publicly available through the Gulf of Mexico Research Initiative Information and Data Cooperative (GRIIDC) at https://data.gulfresearchinitiative.org (https://doi.org/10.7266/N7BZ63Z7))

suggesting deep hydrocarbon seeps are major deep-ocean DOC sources and the prevalence of hydrocarbon seeps in deep Gulf of Mexico (MacDonald et al. 2015; Pohlman et al. 2009, 2010). These data instead suggest that while seep DOC fluxes with very negative Δ^{14}C values may be locally significant, this seep DOC does not appear to accumulate at substantial levels in the deep Gulf of Mexico basin.

An exception to these otherwise "normal" ocean DOC isotopic profiles is observed at several deep sites (>750 m) nearest the Macondo wellhead (Station P3). Here, concentrations of DOC abruptly increase by 8–9 μM (~20–25%). At the same depths, both the δ^{13}C and Δ^{14}C compositions decrease significantly (Fig. 10.3). Using isotopic mass balance of a binary mixing model, the added DOC required δ^{13}C values to be −44.6‰ and −30.8‰ at 1000 m and 1250 m, respectively. Radiocarbon content (as Δ^{14}C) of the added DOC was determined to be −965‰ and −1000‰ at 1000 m and 1250 m depth. The Δ^{14}C values of the added DOC indicate a petrocarbon source; the stable isotopic compositions at each depth represent a 42%:58% mixture of petroleum and methane at 1000 m and an 89%:11% mixture of petroleum and methane at 1250 m.

The presence of a persistent DOC petrocarbon plume, detected some 4 years after DWH near the Macondo wellhead site, is remarkable. The isotope signature of this DOC petrocarbon, however, is unmistakable. At the time of sampling, there was no measurable methane in the water column (Walker et al. 2017, supplemental information), and the presence of petroleum in the water samples in filtered vs. unfiltered replicates was not visually or isotopically perceptible. In addition, the methods used in the Walker study do not isolate methane carbon (only nonvolatile DOC). Thus, Walker and co-workers suggested that immediately following DWH, pre-aged "new" DOC was added following an intense microbial transformation of mesopelagic DWH oil and methane into a natural population of recalcitrant DOC molecules. It is likely this DOC petrocarbon signature will continue to persist until advection eventually "mixes out" this material with background DOC. Until that time, the DOC petrocarbon isotopic anomaly represents a novel geochemical tracer for ultimately further understanding the persistence and biogeochemistry of DOC in the Gulf of Mexico.

10.4.2 Sinking Particulate Organic Carbon

Marine snow is an aggregation of organic and inorganic debris including bacteria, phytoplankton feces, feeding webs, detrital material, biominerals, and lithogenic particles (Passow et al. 2012; Giering et al. 2018). These components are often bound together by ~~a~~ sticky substances called transparent exopolymer particles (TEP), which are produced by phytoplankton, frequently at the final stage of diatom blooms (Passow 2004). The presence of TEP can increase the flocculation of diatom cells by tenfold, and the process accumulates dissolved substances from the water column (Passow 2004). Initially upon formation, TEP is buoyant but, following some degree of decomposition, will begin to sink (Azetsu-Scott and Passow 2004; Giering et al. 2018). Aggregations of foraminifera and radiolarians can also be mucus-rich and sticky (Geiring et al. 2018) binding components. In addition to incorporating dissolved organic matter into marine snow via TEP formation, these particulate accumulations can accumulate hydrophobic materials such as contaminants, including oil residues and PAHs (Giering et al. 2018; Yan et al. 2016; Broman et al. 1987; Lipiotou et al. 1993). When this material sediments out, and reaches the seafloor, it is referred to as marine oil snow sedimentation and flocculent accumulation (MOSSFA), a term coined at a GoMRI (Gulf of Mexico Research Initiative)-sponsored meeting.

Thus, in a direct manner, as it cleanses the water column of contaminants, marine snow also samples the water column for contaminants. Sediment traps serve as monitors of water column contamination and changes therein. Yan et al. (2016) offer direct evidence of the “scrubbing effect” of rapidly sinking diatom aggregations scavenging suspended substances and particles from the spill. Over a 3-month period, the barium contribution to the particulate flux decreased from some 1000 mg/kg of dry weight during the sedimentation event associated with the bloom to 400 mg/kg but then rebounded to 1200 mg/kg afterward. This temporary cleansing action was also reflected in the $\Delta^{14}C$ of the particulates which went from positive values in the bloom to the most negative values observed as Ba increased, reflecting the renewed input in the fossil carbon and oil-derived materials to the particulate flux. It was hypothesized that following the cleansing event, lateral advection renewed contamination of the water column above the sediment trap, causing the increase in deposition of contaminants. At the sinking rates of marine snow, it can be transported laterally to a great distance before it falls; thus the placement of material on the seafloor or in a sediment trap does not correspond with its surface formation site (Diercks et al. 2018).

Chanton et al. (2018) and Geiring et al. (2018) reported the flux and isotopic composition of sinking particles at three sites in the northern Gulf of Mexico following the oil spill and characterized the return of the POM_{sink} flux toward baseline values. The sediment trap at the DWH site (28°40′N, 88°21.6′W; at 1660 m depth) was about 5 km from the DWH site and was impacted by the oil discharge. Sample collection is reported from August 2010 to March 2015 (see also Yan et al. 2016). The reference site (AT357; see Fisher et al. 2014) was at 27°31.5 N (89°42.6 W; at 1160 m depth) and collected from April 2012 through August 2014. The third study site was a seep site, GC-600 (27°22.5′N, 90°30.7′W; at 1380 m depth). The seep frequently exhibits extensive oil slicks on the sea surface above it (MacDonald et al. 1993, 2015; Garcia-Pineda et al. 2013). Sample collection is reported from April 2012 to March 2016. Neither of the latter sites were visibly impacted by hydrocarbons from the DWH spill (Fisher et al. 2014).

Time-series isotope results for POM_{sink} at the DWH; reference and seep sites are depicted in Fig. 10.4 (Chanton et al. 2018). Here, $\Delta^{14}C$ varied from −180‰ to 93‰ at the DWH site, −52‰ to 66‰ at the reference site, and −200‰ to 62‰ at the seep site. In general, following an initial plankton bloom in August 2010, both $\Delta^{14}C$ and $\delta^{34}S$ at the DWH site were isotopically depleted, due to the influence of petro-

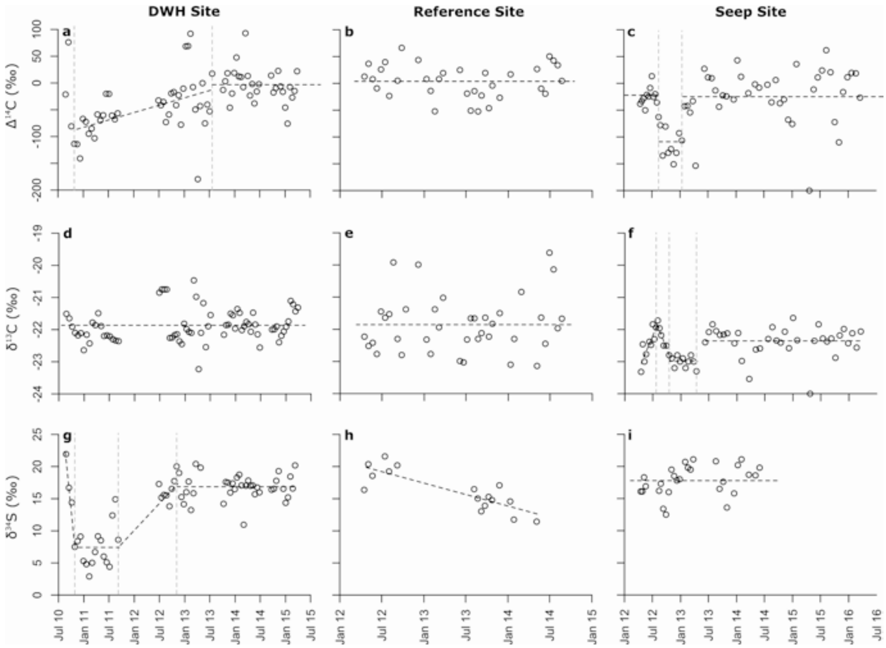

Fig. 10.4 Isotopic results on POM_{sink} for the three sites collected in sediment traps moored above the seafloor (Chanton et al. 2018; Giering et al. 2018). Trends in the time-series data for $\delta^{13}C$, $\Delta^{14}C$, and $\delta\ ^{34}S$ at the three sites were assessed with the *envcpt* function of the R package *EnvCpt* (Killick et al. 2016). This analysis fits a best model fit to the data across time and identifies any change points if they are present. When change points were located, a piecewise simple linear regression was performed between them (Chanton et al. 2018). (Data are publicly available through the Gulf of Mexico Research Initiative Information and Data Cooperative (GRIIDC) at https://data.gulfresearchinitiative.org, https://doi.org/10.7266/N737775J. Reproduced from Elementa (Chanton et al. 2018))

carbon from the wellhead and possibly due to increased terrestrial organic matter input to the site. The most depleted DWH site values observed are given in Table 10.1. The $\Delta^{14}C$ values increased until July 2013, at which time they became relatively constant suggesting background or ambient values had been reached. The $\delta^{34}S$ values followed a similar pattern, leveling off toward presumed background in late 2012, at which time they became similar to the reference site values. Baseline isotopic values are indicated for these two sites, $\Delta^{14}C$‰ −3.2 ± 31.0 and 3.8 ± 31.1, while $\delta^{34}S$ values were 16.9 ± 2.0 and 16.2 ± 3.1 for the DWH and reference site respectively. Carbon-13 values for the two sites did not show any trends and were −21.9‰ ± 0.5 and −21.9‰ ± 0.9, respectively. Relative to these two sites, DWH post July 2013 and reference, seep site values were somewhat depleted for ^{14}C and ^{13}C, especially during a "trough" period when the sediment trap appeared to sample petrocarbon-rich particles from a natural oiled-sedimentation event (Fig. 10.4 and Giering et al. 2018; Chanton et al. 2018). However ^{34}S values did not reflect petrocarbon input at the seep site suggesting that the petrocarbon had been assimilated

Table 10.1 Isotopic values of POM_{susp} over collection intervals at different sites and times

	Isotope values		
Site, condition	Δ^{14}C‰	δ^{13}C‰	δ^{34}S‰
DWH site, depleted values 8 December 2010	−141.0	−22.1	9.1
DWH site, after July 2013	−3.2 ± 31.0	−21.9 ± 0.5	16.9 ± 2.0
Reference site, average	3.8 ± 31.1	−21.9 ± 0.9	16.2 ± 3.1
Seep site, non-trough	−21.7 ± 45.7	−22.3 ± 0.5	18.4 ± 2.1
Seep site, trough	−109.0 ± 29.1	−23.0 ± 0.2	16.6 ± 2.3

For the DWH site, the 2010 values indicate effects from the oil spill, while a return to background is indicated after July 2013. The reference site is similar to the post 2013 DWH site values, confirming this hypothesis. At the seep site, "trough" conditions indicate the capture of a possible natural MOSSFA event in the sediment trap, while non-trough values are more background-like but still somewhat depleted possibly due to seep site influence
Chanton et al. (2018)

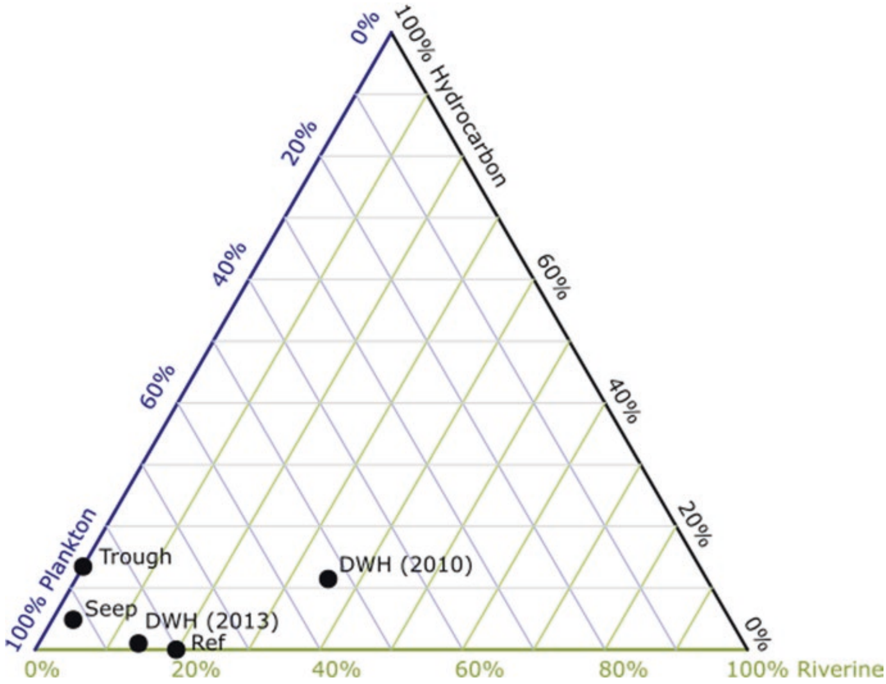

Fig. 10.5 The relative importance of differing carbon sources to sinking particulates in the northern Gulf of Mexico determined from a three end-member model. (Data from Chanton et al. 2018). The importance of marine photosynthetic production is clearly indicated relative to seep and riverine (terrestrial) inputs

by microbes and had entered the food web and subsequently incorporated into marine oil snow (Daly et al. 2016; Passow and Hetland 2016; Passow and Ziervogel 2016). Using a mixing model, Chanton et al. (2018) determined the relative importance of differing carbon sources to the POM_{sink} of the northern Gulf (Fig. 10.5). The model clearly indicated the importance of marine in situ production in all cases.

10.4.3 Sedimentary Organic Carbon

Marine oil snow (MOS) accumulated on the seafloor as far as 120–180 km from the wellhead and was observed to the SW and NE of the wellhead (Romero et al. 2015, 2017; Chanton et al. 2015; Valentine et al. 2014; Stout et al. 2017). As described above, the petrocarbon-affected sediment is referred to as the marine oil snow sedimentation and flocculent accumulation (MOSSFA). The sedimented oil could have been derived from oil that floated on the surface of the Gulf (MacDonald et al. 2015; Daly et al. 2016) or it could have been derived from the deep-sea plume that was focused to the southwest of the wellhead (Valentine et al. 2014; Daly et al. 2016, Mason et al. 2014). Consensus is that the MOSSFA layer was roughly a cm in thickness (Valentine et al. 2014; Brooks et al. 2015; Chanton et al. 2015; Romero et al. 2015).

Radiocarbon ($\Delta^{14}C$) measurements on the surface layers of sediments surrounding the oil spill site collected from 2010 to 2012 indicated the deposition of petrocarbon on the seafloor in a region of 2.4×10^{10} m^2 (Fig. 10.6, Chanton et al.

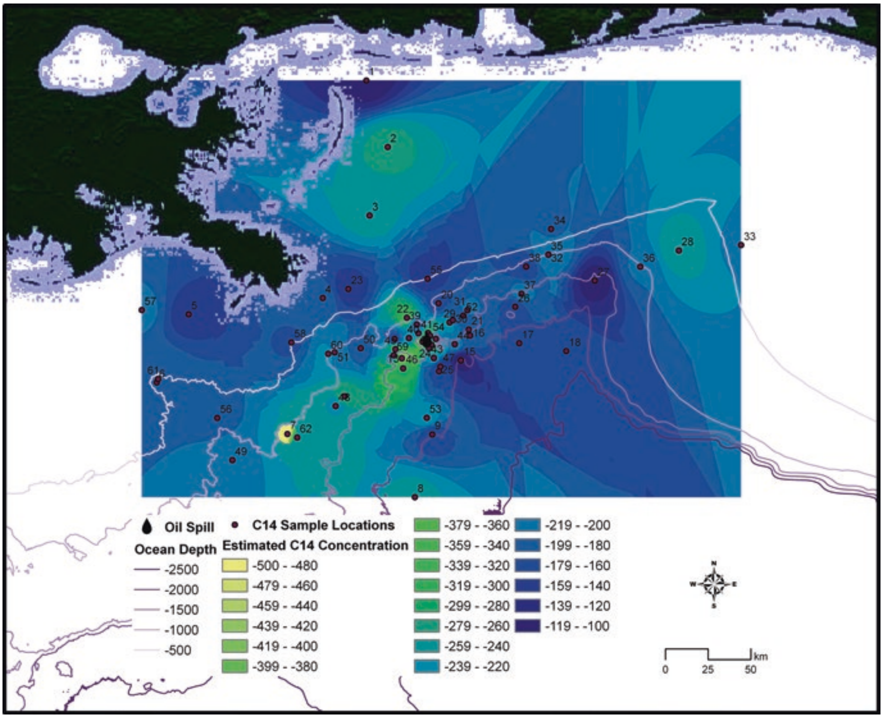

Fig. 10.6 Seafloor radiocarbon map. Points represent the 0–1 cm interval of surface sediments. Data were contoured with the inverse distance weighting (IDW) method and, within the black polygon, the surface area of each 20‰ interval calculated for the seafloor. (Reproduced from Chanton et al. 2015. Data are publicly available through the Gulf of Mexico Research Initiative Information and Data Cooperative (GRIIDC) at https://data.gulfresearchinitiative.org, UDI, R1.x138.078:0024. Reprinted with permission from Chanton et al. 2015. Copyright 2015 American Chemical Society)

2015). The amount of petrocarbon was estimated to be between 0.5% and 9.1% of the quantity of fossil carbon released with a best estimate of 3.0–4.9%. Surface values varied from −500‰ to −107‰ across the area. Background surface values were determined to be −200 ± 29‰ based on values underlying the contaminated sediments. The mean value for surface sedimentary organic matter was determined to be −21.5 ± 0.8‰, indistinguishable from compiled pre-spill surface sediment values for the Gulf of Mexico reported by Rosenheim et al. (2016) of −21.4 ± 1.9‰.

10.4.4 Ramped Pyrolysis-Oxidation of Sedimentary Organic Matter

Ramped pyrolysis-oxidation (Ramped PyrOx or RPO) analysis of the bulk organic matter followed by isotopic analysis of pyrolysates is helpful to gain further insight into how the oil pollution qualitatively changes in terms of thermochemical stability after release into the environment. Early work showed that samples with high polycyclic aromatic hydrocarbon (PAH, a type of compound released by petroleum in the environment and by burning of organic material) concentrations also had lower temperatures of pyrolysis in samples taken soon after the DWH spill from Barataria Bay, Louisiana (Pendergraft et al. 2013). As oil persisted in different forms in beach and marsh environments, compounds containing high amounts of petrocarbon gradually became more stable (Pendergraft and Rosenheim 2014), as indicated by higher temperature intervals registering depleted $\Delta^{14}C$ signatures through time. The shift from volatile (low pyrolysis temperatures) to stable (high pyrolysis temperatures) likely represents a suite of different chemical reactions; the chemical information in RPO analysis is simplified to pyrolysis temperature by nature of rapid combustion of the pyrolysates in preparation for isotopic analysis. Rogers et al. (2019) have recently reported on RPO analysis of deep Gulf sediments in a time series analysis.

In the open ocean, SOM petrocarbon transformations were captured by decreasing concentrations of PAH through time and space (Adhikari et al. 2016). Analysis of a suite of SOM samples in the Gulf of Mexico yielded little evidence for preservation of petrocarbon signatures far from the wellhead site. In fact, weathering stabilization of the petrocarbon is evidenced in deep-sea samples where the petrocarbon signal is still viable (Adhikari et al. 2016) because the strongest $\Delta^{14}C$ depletions are observed at the highest pyrolysis temperatures. However, at sites with low PAH concentrations, there is little evidence of radiocarbon depletion anywhere in the thermochemical reactivity spectrum. This can either be interpreted as full weathering of any petrocarbon signal through complete remineralization or absence of a petrocarbon pulse due to patchiness of the spill's projection in seafloor sediments at distances beyond a few km. Alternatively, the petrocarbon could have been resuspended and advected downslope (Diercks et al. 2018).

10.5 Conclusions and Baselines

An interesting and, perhaps, overlooked aspect of the work summarized in this chapter is the persistence of a water column isotopic signature of the DWH oil spill. For several years, during which there is evidence for degradation of the petrocarbon signature in SOM (Adhikari et al. 2016), water column DOM retained a petrocarbon signature. Whereas much effort has continued to model and measure surface mesoscale transportation processes (Olascoaga and Haller 2012; Poje et al. 2014; Olascoaga et al. 2013; Beron-Verra et al. 2015), comparatively little research has aimed to ascertain midlevel mesopelagic transport processes. In addition to the question of *who* (what microbial populations) were responsible for the transformation of petroleum and methane to DOC, the question of *how* this signature persisted for at least 4 years after the spill is withstanding and potentially illustrative of mid-ocean transport processes near the continental margin. The FTICR-MS data indicate that the DOM became increasingly oxygenated (via photooxidation and biodegradable processes) over time, and this may have led to this persistence.

From trajectories of isotopic values over time, and from spatial variations in isotopic compositions, the research discussed in this chapter has provided estimates of background isotopic values of organic matter pools prior to the oil spill. Baseline DOC isotopic composition in the deep Gulf (P4; >1000 m) appears to vary between −459 and −449‰ for $\Delta^{14}C$ and −21.3 to −21.8‰ for $\delta^{13}C$. For POM_{sink}, background $\Delta^{14}C$ values vary between −30 and +30‰, whereas $\delta^{13}C$ values vary between −21 and −23‰, and $\delta^{34}S$ varies from 13‰ to 20‰. Background values for sedimentary organic matter were −200 ± 29‰ for $\Delta^{14}C$ and 21.4 ± 1.9‰ for $\delta^{13}C$.

Funding Information This research was made possible by grants from the Gulf of Mexico Research Initiative through its consortia: the Center for the Integrated Modeling and Analysis of the Gulf Ecosystem (C-IMAGE), Ecosystem Impacts of Oil and Gas Inputs to the Gulf (ECOGIG), Deep Sea to Coast Connectivity in the Eastern Gulf of Mexico (Deep-C), and the Consortium for Advanced Research of Transport of Hydrocarbon in the Environment (CARTHE). We also acknowledge funding from an American Chemical Society (ACS) Petroleum Research Fund (PRF) New Directions (ND) grant (to B.D.W).

References

Adhikari PL, Maiti K, Overton EB, Rosenheim BE, Marx BD (2016) Distributions and accumulation rates of polycyclic aromatic hydrocarbons in the northern Gulf of Mexico sediments. Environ Pollut 212:413–423. https://doi.org/10.1016/j.envpol.2016.01.064

Arnosti C, Repeta DJ, Blough NV (1994) Rapid bacterial degradation of polysaccharides in anoxic marine systems. Geochim Cosmochim Acta 58:2639–2652. https://doi.org/10.1016/0016-7037(94)90134-1

Aycard M, Derenne S, Largeau C, Mongenot T, Tribovillard N, Baudin F (2003) Formation pathways of proto-kerogens in Holocene sediments of the upwelling influenced Cariaco Trench, Venezuela. Org Geochem 34:701–718. https://doi.org/10.1016/S0146-6380(03)00058-5

Azetsu-Scott K, Passow U (2004) Ascending marine particles: significance of transparent exopolymer particles (TEP) in the upper ocean. Limnol Oceanogr 49(3):741–748. https://doi.org/10.4319/lo.2004.49.3.0741

Bae E, Yeo IJ, Jeong B, Shin Y, Shin KH, Kim S (2011) Study of double bond equivalents and the numbers of carbon and oxygen atom distribution of dissolved organic matter with negative-mode FT-ICR MS. Anal Chem 83:4193–4199. https://doi.org/10.1021/ac200464q

Bauer JE, Williams PM, Druffel ER (1992) 14C activity of dissolved organic carbon fractions in the north-central Pacific and Sargasso Sea. Nature, 357(6380), 667

Bauer JE, Druffel ERM, Wolgast DM, Griffin S (2002) Temporal and regional variability in sources and cycling of DOC and POC in the northwest Atlantic continental shelf and slope. Deep Sea Res II 49:4387–4419

Beaupre SR, Druffel ERM, Griffin G (2007) A low-blank photochemical extraction system for concentration and isotopic analyses of marine dissolved organic carbon. Limnol Oceanogr Methods 5(6):174–184

Benner R, Pakulski JD, Mccarthy M, Hedges JI, Hatcher PG (1992) Bulk chemical characteristics of dissolved organic matter in the ocean. Science 255:1561–1564. https://doi.org/10.1126/science.255.5051.1561

Beron-Vera FJ, Olascoaga MJ, Haller G, Farazmand J, Wang TY (2015) Dissipative inertial transport patterns near coherent Lagrangian eddies in the ocean. Interdiscip J Nonlinear Sci 25:8

Bosman SH, Chanton JP, Rogers KL (2017) Using stable and radiocarbon analyses as a forensic tool to find evidence of oil in the particulates of the water column and on the seafloor following the 2010 Gulf of Mexico Oil Spill. In: Stout S, Wang Z (eds) Oil spill environmental forensics case studies. Butterworth and Heinemann, Cambridge, MA, pp 639–650

Broman D, Colmsjö A, Ganning B, Näf C, Zebühr Y, Östman C (1987) "Fingerprinting" petroleum hydrocarbons in bottom sediment, plankton, and sediment trap collected seston. Mar Pollut Bull 18(7):380–388. https://doi.org/10.1016/0025-326X(87)90317-1

Brooks GR, Larson RA, Schwing PT, Romero I, Moore C, Reichart GJ, Jilbert T, Chanton JP, Hastings DW, Overholt WA, Marks KP, Kostka JE, Homes CW, Hollander D (2015) Sedimentation pulse in the NE Gulf of Mexico following the 2010 DWH blowout. PLoS One 10(7):e0132341. https://doi.org/10.1371/journal.pone.0132341

Burdige DJ, Gardner KG (1998) Molecular weight distribution of dissolved organic carbon in marine sediment pore waters. Mar Chem 62:45–64. https://doi.org/10.1016/S0304-4203(98)00035-8

Burdige DJ, Komada T (2015) Sediment pore waters. In: Hansell DA, Carlson CA (eds) Biogeochemistry of marine dissolved organic matter, 2nd edn. Academic Press, New York. pp 535–577

Chanton J, Zhao T, Rosenheim BE, Joye S, Bosman S, Brunner C, Yeager KM, Diercks AR, Hollander D (2015) Using natural abundance radiocarbon to trace the flux of petrocarbon to the seafloor following the Deepwater Horizon oil spill. Environ Sci Technol 49(2):847–854

Chanton JP, Giering SL, Bosman SH, Rogers KL, Sweet J, Asper VL, Diercks AR, Passow U (2018) Isotopic composition of sinking particles: oil effects, recovery and baselines in the Gulf of Mexico, 2010–2015. Elementa Sci Anthropocene 6(43):1–19

Chen M, Hur J (2015) Pre-treatments, characteristics, and biogeochemical dynamics of dissolved organic matter in sediments: a review. Water Res 79:10–25. https://doi.org/10.1016/j.watres.2015.04.018

Daly KL, Passow U, Chanton J, Hollander D (2016) Assessing the impacts of oil-associated marine snow formation and sedimentation during and after the Deepwater Horizon oil spill. Anthropocene 13:18–33. https://doi.org/10.1016/j.ancene.2016.01.006

Davis JE (2017) The Gulf: the making of an American Sea. Liveright Publishing, New York

Diercks AR, Asper VL (1997) In situ settling speeds of marine snow aggregates below the mixed layer: Black Sea and Gulf of Mexico. Deep Sea Res Part I 44(3):385–398. https://doi.org/10.1016/S0967-0637(96)00104-5

Diercks AR, Dike C, Asper V, DiMarco SF, Chanton J, Passow U (2018) Scales of seafloor sediment resuspension in the northern Gulf of Mexico. Elementa: Science of the Anthropocene, 6(32) http://doi.org/10.1525/elementa.285

Dittmar T, Stubbins A (2013) Dissolved organic matter in aquatic systems, 2nd edn. Elsevier Ltd., New York

Dittmar T, Koch B, Hertkorn N, Kattner G (2008) A simple and efficient method for the solid-phase extraction of dissolved organic matter (SPE-DOM) from seawater. Limnol Oceanogr Methods 6:230–235. https://doi.org/10.4319/lom.2008.6.230

Druffel ERM, Williams PM, Bauer JE, Ertel JR (1992) Cycling of dissolved and particulate organic matter in the open ocean. J Geophys Res 97(C10):15639–15659. https://doi.org/10.1029/92JC01511

Druffel ERM, Bauer JE, Williams PM, Griffin S, Wolgast D (1996) Seasonal variability of particulate organic radiocarbon in the northeast Pacific Ocean. J Geophys Res 101(C9):20543–20552. http://dx.doi.org/10.1029/96JC01850

Druffel ERM, Griffin S, Coppola AI, Walker BD (2016) Radiocarbon in dissolved organic carbon of the Atlantic Ocean. Geophys Res Lett 43(10):5279–5286

Emerson S, Hedges JI (1988) Processes controlling the organic carbon content of open ocean sediments. Paleogeogr Paleoclimatol Paleoecol 3:621–634. https://doi.org/10.1029/PA003i005p00621

Fisher CR, Hsing P-Y, Kaiser CL, Yoerger DR, Roberts HH, Shedd WW, Cordes EE, Shank TM, Verlet SP, Saunders MG, Larcom EA, Brooks JM (2014) Footprint of Deepwater Horizon blowout impact to deep-water coral communities. Proc Natl Acad Sci U S A 111(32):11744–11749. https://doi.org/10.1073/pnas.1403492111

Garcia-Pineda O, MacDonald I, Hu C, Svejkovsky J, Hess M, Dukhovskoy D, Morey SL (2013) Detection of floating oil anomalies from the Deepwater Horizon oil spill with synthetic aperture radar. Oceanography 26:124–137. https://doi.org/10.5670/oceanog.2013.38

Giering SLC, Yan B, Sweet J, Asper V, Diercks A, Chanton J, Passow U (2018) The ecosystem baseline for particle flux in the Northern Gulf of Mexico. Elementa Sci Anthropocene 6(1):6. https://doi.org/10.1525/elementa.264

Hansell DA (2013) Recalcitrant dissolved organic carbon fractions. Annu Rev Mar Sci 5:421–445. https://doi.org/10.1146/annurev-marine-120710-100757

Hansell DA, Carlson CA, Repeta DJ, Schlitzer R (2009) Dissolved organic matter in the ocean—A controversy stimulates new insights. Oceanography 22(4):202–211

Hedges JI (1978) The formation and clay mineral reactions of melanoidins. Geochim Cosmochim Acta 42:69–76. https://doi.org/10.1016/0016-7037(78)90218-1

Hedges JI (1992) Global biogeochemical cycles: progress and problems. Mar Chem 39:67–93. https://doi.org/10.1016/0304-4203(92)90096-S

Hedges JI, Keil RG (1995) Sedimentary organic matter preservation: an assessment and speculative synthesis. Mar Chem 49:137–139. https://doi.org/10.1016/0304-4203(95)00013-H

Helms JR (2012) Spectroscopic characterization of dissolved organic matter: insights into composition photochemical transformation and carbon cycling. Dissertation, Old Dominion University

Henrichs SM (1992) Early diagenesis of organic matter in marine sediments: progress and perplexity. Mar Chem 39:119–149. https://doi.org/10.1016/0304-4203(92)90098-U

Hertkorn N, Benner R, Frommberger M, Schmitt-Kopplin P, Witt M, Kaiser K, Kettrup A, Hedges JI (2006) Characterization of a major refractory component of marine dissolved organic matter. Geochim Cosmochim Acta 70:2990–3010. https://doi.org/10.1016/j.gca.2006.03.021

Jaggi A (2018) Dissolved organic matter in marine environments: a study of the origin lability and molecular composition. Dissertation, University of Calgary

Kim S, Kaplan LA, Benner R, Hatcher PG (2004) Hydrogen-deficient molecules in natural riverine water samples - evidence for the existence of black carbon in DOM. Mar Chem 92:225–234. https://doi.org/10.1016/j.marchem.2004.06.042

Killick R, Beaulieu C, Taylor S. 2016. EnvCpt: Detection of Structural Changes in Climate and Environment Time Series. R package version 0.1.1. https://CRAN.Rproject.org/package=EnvCpt

Koch BP, Witt M, Engbrodt R, Dittmar T, Kattner G (2005) Molecular formulae of marine and terrigenous dissolved organic matter detected by electrospray ionization Fourier transform ion cyclotron resonance mass spectrometry. Geochim Cosmochim Acta 69:3299–3308. https://doi.org/10.1016/j.gca.2005.02.027

Koch BP, Dittmar T, Witt M, Kattner G (2007) Fundamentals of molecular formula assignment to ultrahigh resolution mass data of natural organic matter. Anal Chem 79:1758–1763. https://doi.org/10.1021/ac061949s

Kujawinski EB, Hatcher PG, Freitas MA (2002) High-resolution fourier transform ion cyclotron resonance mass spectrometry of humic and fulvic acids: improvements and comparisons. Anal Chem 74:413–419. https://doi.org/10.1021/ac0108313

Libes S (2011) Introduction to marine biogeochemistry. Academic Press, New York

Lipiatou E, Marty J-C, Saliot A (1993) Sediment trap fluxes of polycyclic aromatic hydrocarbons in the Mediterranean Sea. Mar Chem 44(1):43–54. https://doi.org/10.1016/0304-4203(93)90005-9

MacDonald IR, Guinasso NL Jr, Acchleson SG, Amos JF, Duckworth R, Sassen R, Brooks JM (1993) Natural oil slicks in the Gulf of Mexico visible from space. J Geophys Res 98:16351–16364

MacDonald IR, Garcia-Pineda O, Beet A, Daneshgar Asl S, Feng L, Graettinger G, French-McCay D, Holmes J, Hu C, Huffer F, Leifer I, Muller-Karger F, Solow A, Silva M, Swayze G (2015) Natural and unnatural oil slicks in the Gulf of Mexico. J Geophys Res Oceans 120:8364–8380. https://doi.org/10.1002/2015JC011062

Mason OU, Scott NM, Gonzalez A, Robbins-Pianka A, Bælum J, Kimbrel J, Bouskill NJ, Prestat E, Borglin S, Joyner DC, Fortney JL, Jurelevicius D, Stringfellow WT, Alvarez-Cohen L, Hazen TC, Knight R, Gilbert JA, Jansson JK (2014) Metagenomics reveals sediment microbial community response to Deepwater Horizon oil spill. Int Soc Microb Ecol J 8(7):464–1475

Mentges A, Feenders C, Seibt M, Blasius B, Dittmar T (2017) Functional molecular diversity of marine dissolved organic matter is reduced during degradation. Front Mar Sci 4:1–10. https://doi.org/10.3389/fmars.2017.00194

Nebbioso A, Piccolo A (2013) Molecular characterization of dissolved organic matter (DOM): a critical review. Anal Bioanal Chem 405:109–124. https://doi.org/10.1007/s00216-012-6363-2

Ogawa H, Amagai Y, Koike I, Kaiser K, Benner R (2001) Production of refractory dissolved organic matter by bacteria. Science 292:917–920. https://doi.org/10.1126/science.1057627

Olascoaga MJ, Haller G (2012) Forecasting sudden changes in environmental pollution patterns. Proc Natl Acad Sci U S A 109(13):4738–4743

Olascoaga MJ, Beron-Vera FJ, Haller G, Triñanes J, Iskandarani M, Coelho EF, Haus BK, Huntley HS, Jacobs G, Kirwan AD Jr, Lipphardt BL Jr, Özgökmen TM, Reniers AJHM, Valle-Levinson A (2013) Drifter motion in the Gulf of Mexico constrained by altimetric Lagrangian coherent structures. Geophys Res Lett 40(23):6171–6175

Opsahl S, Benner R, Amon RMW (1999) Major flux of terrigenous dissolved organic matter through the Arctic Ocean. Limnol Oceanogr 44:2017–2023. https://doi.org/10.4319/lo.1999.44.8.2017

Passow U (2004) Switching perspectives: do mineral fluxes determine particulate organic carbon fluxes or vice versa? Geochem Geophys Geosyst 5(4):Q04002. https://doi.org/10.1029/2003GC000670

Passow U, Hetland RD (2016) What happened to all of the oil? Oceanography 29(3):88–95. https://doi.org/10.5670/oceanog.2016.73

Passow U, Ziervogel K (2016) Marine snow sedimented oil released during the Deepwater Horizon spill. Oceanography 29(3):118–125. https://doi.org/10.5670/oceanog.2016.76

Passow U, Ziervogel K, Asper V, Diercks A (2012) Marine snow formation in the aftermath of the Deepwater Horizon oil spill in the Gulf of Mexico. Environ Res Lett 7(3):1–11. https://doi.org/10.1088/1748-9326/7/3/035301

Pendergraft MA, Rosenheim BE (2014) Varying relative degradation rates of oil in different forms and environments revealed by ramped pyrolysis. Environ Sci Technol 48(18):10966–10974. https://doi.org/10.1021/es501354c

Pendergraft MA, Dincer Z, Sericano JL, Wade TL, Kolasinski J, Rosenheim BE (2013) Linking ramped pyrolysis isotope data to oil content through PAH analysis. Environ Res Lett 8:1–10. https://doi.org/10.1088/1748-9326/8/4/044038

Pohlman JW, Bauer JE, Canuel EA, Grabowski KS, Knies DL, Mitchell CS, Whiticar MJ, Coffin RB (2009) Methane sources in gas hydrate-bearing cold seeps: evidence from radiocarbon and stable isotopes. Mar Chem 115:102–109. https://doi.org/10.1016/j.marchem.2009.07.001

Pohlman JW, Bauer JE, Waite WF, Osburn CL, Chapman NR (2010) Methane hydrate-bearing seeps as a source of aged dissolved organic carbon to the oceans. Nat Geosci 4:37–41. https://doi.org/10.1038/ngeo1016

Poje AC, Özgökmen TM, Lipphart BL, Haus BK, Ryan EH, Haza AC, Jacobs GA, Reniers AJHM, Olascoaga MJ, Novelli G, Griffa A, Beron-Vera FJ, Chen SS, Coelho E, Hogan PJ, Kirwan AD Jr, Huntley HS, Mariano AJ (2014) Submesoscale dispersion in the vicinity of the Deepwater Horizon spill. Proc Natl Acad Sci U S A 111(35):12693–12698

Rivas D, Badan A, Ochoa J (2005) The ventilation of the deep Gulf of Mexico. J Phys Oceanogr 35:1763–1781

Rogers KL, Bosman SH, Lardie-Gaylord M, McNichol A, Rosenheim BE, Montoya JP, Chanton JP (2019) Petrocarbon evolution: Ramped pyrolysis/oxidation and isotopic studies of contaminated oil sediments from the Deepwater Horizon oil spill in the Gulf of Mexico. PloS one 14(2): e0212433

Romero IC, Schwing PT, Brooks GR, Larson RA, Hastings DW, Ellis G, Goddard EA, Hollander DJ (2015) Hydrocarbons in deep-sea sediments following the 2010 Deepwater Horizon blowout in the northeast Gulf of Mexico. PLoS One 10(5):e0128371

Romero IC, Toro-Farmer G, Diercks A-R, Schwing P, Muller-Karger F, Murawski S, Hollander DJ (2017) Large-scale deposition of weathered oil in the Gulf of Mexico following a deep-water oil spill. Environ Pollut 228:179–189. https://doi.org/10.1016/j.envpol.2017.05.019

Rosenheim BE, Pendergraft MA, Flowers GC, Carney R, Sericano J, Amer RM, Chanton J, Dincer A, Wade TL (2016) Employing extant stable carbon isotope data in Gulf of Mexico sedimentary organic matter for oil spill studies. Deep Sea Res II 129:249–258

Schmidt F, Koch BP, Witt M, Hinrichs K-UU (2014) Extending the analytical window for water-soluble organic matter in sediments by aqueous Soxhlet extraction. Geochim Cosmochim Acta 141:83–96. https://doi.org/10.1016/j.gca.2014.06.009

Schwing PT, Brooks GR, Larson RA, Holmes CW, O'Malley BJ, Hollander DJ (2017) Constraining the spatial extent of marine oil snow sedimentation and flocculent accumulation (MOSSFA) following the Deepwater Horizon event using an excess 210Pb flux approach. Environ Sci Technol 51(11):5962–5968. https://doi.org/10.1021/acs.est.7b00450

Sleighter RL, Hatcher PG (2008) Molecular characterization of dissolved organic matter (DOM) along a river to ocean transect of the lower Chesapeake Bay by ultrahigh resolution electrospray ionization Fourier transform ion cyclotron resonance mass spectrometry. Mar Chem 110:140–152. https://doi.org/10.1016/j.marchem.2008.04.008

Spencer RGM, Aiken GR, Butler KD, Dornblaser MM, Streigl RG (2009) Utilizing chromophoric dissolved organic matter measurements to derive export and reactivity of dissolved organic carbon exported to the Arctic Ocean: a case study of the Yukon River. Alaska Geophys Res Lett 36:1–6. https://doi.org/10.1029/2008GL036831

Stout SA, Rouhani S, Liu B, Oehrig J, Ricker RW, Baker G, Lewis C (2017) Assessing the footprint and volume of oil deposited in deep-sea sediments following the Deepwater Horizon oil spill. Mar Pollut Bull 114(1):327–342. https://doi.org/10.1016/j.marpolbul.2016.09.046

Stubbins A, Dittmar T (2015) Illuminating the deep: molecular signatures of photochemical alteration of dissolved organic matter from North Atlantic Deep Water. Mar Chem 177:318–324. https://doi.org/10.1016/j.marchem.2015.06.020

Stubbins A, Spencer RGM, Chen H, Hatcher PG, Mopper K, Hernes PJ, Mwamba VL, Mangangu AM, Wabakanghanzi JN, Six J (2010) Illuminated darkness: molecular signatures of Congo River dissolved organic matter and its photochemical alteration as revealed by ultrahigh precision mass spectrometry. Limnol Oceanogr 55:1467–1477. https://doi.org/10.4319/lo.2010.55.4.1467

Stuiver M, Polach HA (1977) Reporting Of 14C data. Radiocarbon 19:355–263

Tarr M, Zito P, Overton E, Olson GM, Adhikari AP, Reddy CM (2016) Weathering of oil spilled in the marine environment. Oceanography 29:126–135. https://doi.org/10.5670/oceanog.2016.77

Turley CM, Stutt ED (2000) Depth-related cell-specific bacterial leucine incorporation rates on particles and its biogeochemical significance in the Northwest Mediterranean. Limnol Oceanogr 45:419–425. https://doi.org/10.4319/lo.2000.45.2.0419

Valentine DL, Fisher GB, Bagby SC, Nelson RK, Reddy CM, Sylva SP, Woo MA (2014) Fallout plume of submerged oil from Deepwater Horizon. Proc Natl Acad Sci U S A 111(45):15906–15911. https://doi.org/10.1073/pnas.1414873111

Verschuren D (1993) A lightweight extruder for accurate sectioning of soft-bottom lake sediment cores in the field. Limnol Oceanogr 38:1796–1802. https://doi.org/10.4319/lo.1993.38.8.1796

Vogel JS, Southon JR, Nelson DE (1987) Catalyst and binder effects in the use of filamentous graphite for AMS. Nucl Instrum Methods Phys Res, Sect B 29(1–2):50–56

Wakeham SG, Sinninghe Damsté JS, Kohnen MEL, De Leeuw JW (1995) Organic sulfur compounds formed during early diagenesis in Black Sea sediments. Geochim Cosmochim Acta 59:521–533. https://doi.org/10.1016/0016-7037(94)00361-O

Walker BD, Xu X (2019) An improved method for the sealed-tube zinc graphitization of microgram carbon samples for and 14C AMS measurement. Nucl Instrum Methods Phys Res Sect B 438:58–65. https://doi.org/10.1016/j.nimb.2018.08.004

Walker BD, Druffel ERM, Kolasinski J, Roberts BJ, Xu X, Rosenheim BE (2017) Stable and radiocarbon isotopic composition of dissolved organic matter in the Gulf of Mexico. Geophys Res Lett 44:8424–8434. https://doi.org/10.1002/2017GL074155

Williams PM, Druffel ERM (1987) Radiocarbon in dissolved organic-matter in the Central North Pacific-Ocean. Nature 330(6145):246–248

Xu X, Trumbore SE, Zheng S, Southon JR, McDuffee KE, Luttgen M, Liu JC (2007) Modifying a sealed tube zinc reduction method for preparation of AMS graphite targets: reducing background and attaining high precision. Nucl Instrum Methods Phys Res Sect B 259:320–329. https://doi.org/10.1016/j.nimb.2007.01.175

Yan B, Passow U, Chanton JP, Nöthig E-M, Asper V, Sweet J, Pitiranggon M, Diercks A, De P (2016) Sustained deposition of contaminants from the Deepwater Horizon spill. Proc Natl Acad Sci U S A 113(24):E3332–E3340. https://doi.org/10.1073/pnas.1513156113